

Cite this: *Chem. Sci.*, 2020, **11**, 1905

All publication charges for this article have been paid for by the Royal Society of Chemistry

Received 28th October 2019  
Accepted 4th January 2020

DOI: 10.1039/c9sc05444h  
[rsc.li/chemical-science](http://rsc.li/chemical-science)

## Introduction

Nickel catalysis has the potential to replace palladium catalysis in some reactions and to enable new reactivity that can be exploited in organic synthesis.<sup>1</sup> These reactions include tandem photocatalysis/cross-coupling,<sup>2,3</sup> reductive cross-electrophile coupling,<sup>4</sup> and the cross-coupling of phenol derivatives,<sup>5</sup> aryl fluorides,<sup>6,7</sup> and amides.<sup>8</sup> Several issues remain to be resolved before the full potential and impact of nickel catalysis can be realised. We must understand how nickel interacts with the functional groups that are present in target molecules in the fine chemicals, agrochemicals, and pharmaceutical industries to understand the scope and limitations of existing methods and the opportunities and challenges to consider when developing new ones. The underlying reaction mechanisms in nickel catalysis, and how these depend on substrate and ligand

<sup>a</sup>WestCHEM Department of Pure and Applied Chemistry, University of Strathclyde, 295 Cathedral Street, Glasgow, G1 1XL, Scotland, UK. E-mail: [david.nelson@strath.ac.uk](mailto:david.nelson@strath.ac.uk)

<sup>b</sup>Syngenta, Jealott's Hill International Research Centre, Bracknell, Berkshire, RG42 6EY, UK

† Dedicated to Professor Robert Mulvey on the occasion of his 60th birthday.

‡ All data underpinning this publication are openly available from the University of Strathclyde KnowledgeBase at <https://doi.org/10.15129/0e956fd7-939e-4b60-be15-d530ed0b8b2c>.

§ Electronic supplementary information (ESI) available: rate constants, reaction procedures, characterisation data for compounds, and energies and geometries from DFT studies. See DOI: 10.1039/c9sc05444h.

¶ Current address: Leibniz-Institute for Catalysis, Albert-Einstein-Straße 29a, 18059 Rostock, Germany.

|| Current address: Institute for Chemical Research (IIQ), CSIC-University of Sevilla, Avda. Américo Vespucio 49, 41092 Sevilla, Spain.

## Aldehydes and ketones influence reactivity and selectivity in nickel-catalysed Suzuki–Miyaura reactions†‡§

Alasdair K. Cooper,<sup>a</sup> David K. Leonard,<sup>ID</sup> Sonia Bajo,<sup>||a</sup> Paul M. Burton<sup>b</sup> and David J. Nelson <sup>\*a</sup>

The energetically-favorable coordination of aldehydes and ketones – but not esters or amides – to  $\text{Ni}^0$  during Suzuki–Miyaura reactions can lead either to exquisite selectivity and enhanced reactivity, or to inhibition of the reaction. Aryl halides where the C–X bond is connected to the same  $\pi$ -system as an aldehyde or ketone undergo unexpectedly rapid oxidative addition to  $[\text{Ni}(\text{COD})(\text{dppf})]$  (1), and are selectively cross-coupled during competition reactions. When aldehydes and ketones are present in the form of exogenous additives, the cross-coupling reaction is inhibited to an extent that depends on the strength of the coordination of the pendant carbonyl group to  $\text{Ni}^0$ . This work advances our understanding of how common functional groups interact with  $\text{Ni}^0$  catalysts and how these interactions affect workhorse catalytic reactions in academia and industry.

structure, remain relatively poorly understood compared to palladium catalysis, and so nickel-catalysed reactions are often treated as a 'black box'. Correspondingly, reaction design and optimisation rely heavily on empirical observations.

The mechanisms of nickel-catalysed cross-coupling reactions show a complex dependence on ligand and/or substrate. The mechanistic landscape is further complicated by the often-ambiguous role of nickel(i) species in catalysis.<sup>9–12</sup>  $[\text{Ni}(\text{NHC})_2]$  and  $[\text{Ni}(\text{PR}_3)_4]$  complexes react with aryl halides by oxidative addition or halide abstraction, depending on the ligand and substrate structure.<sup>13–17</sup>  $[\text{Ni}(\text{COD})(\text{dppf})]$  (1)<sup>18</sup> undergoes oxidative addition to aryl halides, followed by rapid comproportionation to form  $[\text{NiX}(\text{dppf})]$  (Fig. 1(a));<sup>19</sup> we have established the

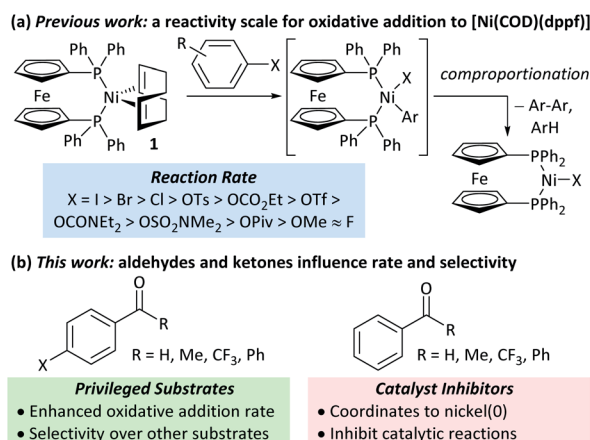


Fig. 1 (a) Previous work. (b) This work.



order of reactivity of a series of aryl (pseudo) halides. It was noted during our previous studies that aryl halides that had aldehyde or ketone substituents underwent unexpectedly fast oxidative addition. Further investigations have revealed that aldehyde and ketone functional groups can act either as directing groups for selective synthesis or as inhibitors of catalytic reactions (Fig. 1(b)). Our initial empirical study showed that various coordinating groups elicit these effects, and that they are considerably more marked for nickel than for palladium.<sup>20</sup> Here, we examine the specific case of aldehydes and ketones in depth using a range of experimental and computational techniques.

## Results and discussion

### Kinetic studies of oxidative addition

Aldehyde and ketone-substituted aryl chlorides undergo surprisingly rapid oxidative addition, compared to the oxidative addition rates for a set of other substrates. The consumption of **1** in the presence of an excess of aryl halide was monitored using  $^{31}\text{P}$  NMR spectroscopy and exhibited pseudo-first order behaviour; rate data are recorded in Table 1. The ultimate nickel-containing products are  $[\text{NiX}(\text{dppf})]$  complexes, as confirmed by EPR and  $^1\text{H}$  NMR spectroscopies.<sup>21</sup> In contrast to cross-coupling reactions (*vide infra*) where transmetalation and reductive elimination can take place, the only pathway available to the arynickel(II) halide intermediates formed during these kinetic experiments is comproportionation with **1** to form  $\text{Ni}^{\text{I}}$  products.

Substrates **2-Cl** to **4-Cl** undergo oxidative addition much more rapidly than electron-deficient aryl chloride **5-Cl** or bromide **5-Br**. These large rate differences cannot be attributed simply to inductive or mesomeric electronic effects; Hammett  $\sigma_p$  is 0.4–0.5 for ketones, aldehydes and esters and 0.54 for trifluoromethyl.<sup>22</sup> The Hammett plot for oxidative addition of aryl chlorides to **1** is shown in Fig. 2.<sup>19</sup>

Ligand exchange, where COD is replaced with the aryl halide, and the oxidative addition event that follows cannot be deconvoluted; we propose that the favourable coordination of aldehydes and ketones to  $\text{Ni}^{\text{I}}$  (*vide infra*) improves the equilibrium position of the ligand exchange (COD *versus* aryl halide), leading to a reaction that is more rapid overall. Consistent with this, signals that are tentatively assigned to an  $\eta^2(\text{CO})$  complex

**Table 1** Pseudo-first order and relative rate constants for the reactions between **1** and substrates **2–6**. All rate constants are the average of two measurements. [nd] = not determined

Substrate	Oxidative addition rate constants		
	$k_{\text{obs}}$ (20 °C)	$k_{\text{obs}}$ (50 °C)	$k_{\text{rel}}$
<b>2a-Cl</b>	$2.5(3) \times 10^{-4} \text{ s}^{-1}$	[nd]	0.32
<b>2b-Cl</b>	$4.2(3) \times 10^{-4} \text{ s}^{-1}$	[nd]	0.54
<b>2c-Cl</b>	$3.0(2) \times 10^{-4} \text{ s}^{-1}$	[nd]	0.38
<b>3-Cl</b>	$1.41(1) \times 10^{-4} \text{ s}^{-1}$	[nd]	0.18
<b>4-Cl</b>	$9.2(2) \times 10^{-5} \text{ s}^{-1}$	[nd]	0.12
<b>5-Cl</b>	[nd]	$2.39(3) \times 10^{-4} \text{ s}^{-1}$	0.007
<b>5-Br</b>	$2.38(4) \times 10^{-5} \text{ s}^{-1}$	$1.02(1) \times 10^{-3} \text{ s}^{-1}$	0.031
<b>5-I</b>	$7.8(1) \times 10^{-4} \text{ s}^{-1}$	[nd]	1.0
<b>6-Cl</b>	[nd]	$1.85(4) \times 10^{-4} \text{ s}^{-1}$	0.005

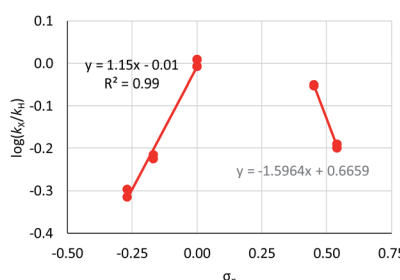


**Fig. 2** Hammett plot for oxidative addition of aryl chlorides to **1** from reactions at 50 °C in benzene- $d_6$ .<sup>19</sup>

are observed during the oxidative addition reactions of **3-Cl**; various complexes of this type are known,<sup>23–30</sup> and have been implicated in nickel-mediated reactions.<sup>31</sup> The observed signals in the  $^{31}\text{P}\{^1\text{H}\}$  NMR spectrum are consistent with a square planar complex (two doublets with  $^2J_{\text{PP}}$  of 31 Hz). This geometry is a result of electron donation from the bisphosphine ligand into the  $3d(x^2-y^2)$  orbital, which is also engaged in d to  $\pi^*$  back-bonding.<sup>32,33</sup> The measured  $K_{\text{eq}}$  for the displacement of COD from **1** using benzaldehyde (>20), benzophenone (0.65), and acetophenone (0.02) are sufficiently large that under catalytic conditions – *i.e.* in the presence of a large excess (*ca.* 10–100 equiv.) of each cross-coupling partner – that this coordination



would be expected to occur to the extent that between 2 and 100% of the  $\text{Ni}^0$  present would be coordinated to a carbonyl group. The lack of a similar effect for esters (e.g. **6-Cl**) is attributed to  $\text{n}$  to  $\pi_{\text{CO}}^*$  resonance effects between the oxygen lone pair and the ester carbonyl group.

### Cross-coupling selectivity

The coordination of aldehydes and ketones to  $\text{Ni}^0$  can be leveraged to achieve selective cross-coupling. Optimised cross-coupling conditions were developed for the prototypical cross-coupling of **2a-Br** with *p*-tolylboronic acid, catalysed by well-defined  $[\text{NiCl}(\text{o-tol})(\text{dppf})]$  pre-catalyst **7**,<sup>34</sup> using factorial experimental design.<sup>§</sup> To dissect the contributions of electronic and coordination effects, experiments were performed in which bromobenzene and a functionalized aryl bromide competed for a limiting amount of boronic acid (Fig. 3(a)).<sup>\*\*</sup> Data were interpreted by quantifying selectivity using eqn (1) (Fig. 3(b)); this has values between  $-1$  and  $+1$  which represent complete selectivity for bromobenzene and functionalised aryl bromide, respectively. The reaction selectivity was plotted *versus*  $\sigma$  (Fig. 3(c)).<sup>35</sup> These data show that selectivity is typically insensitive to the electronic properties of the aryl halide, but significant selectivity is achieved when the aryl halide has a ketone or aldehyde functional group.<sup>36</sup> This selectivity trend is observed for both *meta*- and *para*-substituted aryl bromides. These data confirm that aldehyde and ketone substituents can be used to induce selective cross-coupling at one substrate present within the reaction.

### Computational modelling of ring walking and oxidative addition

DFT calculations give further insights into these reactions.<sup>††</sup>  $[\text{Ni}(\text{dppf})(\eta^2\text{-benzene})]$  (**8**) was assigned  $G_{\text{rel}} = 0$ . Consistent

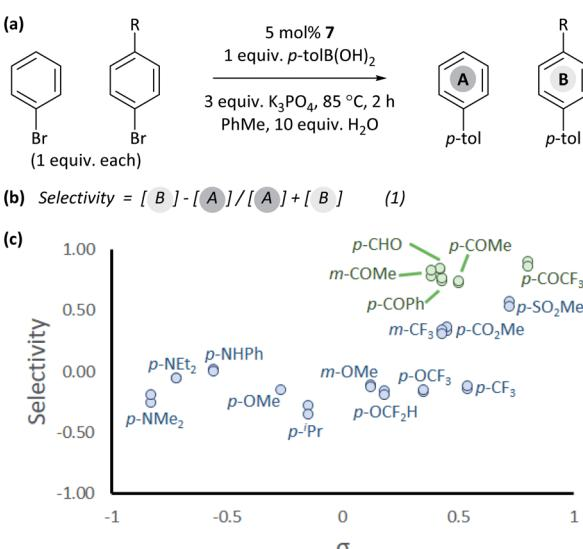


Fig. 3 Competition experiments: (a) reaction conditions; (b) quantification of selectivity; and (c) reactions in toluene with 10 equiv. water. Each individual competition experiment is plotted as a separate point.

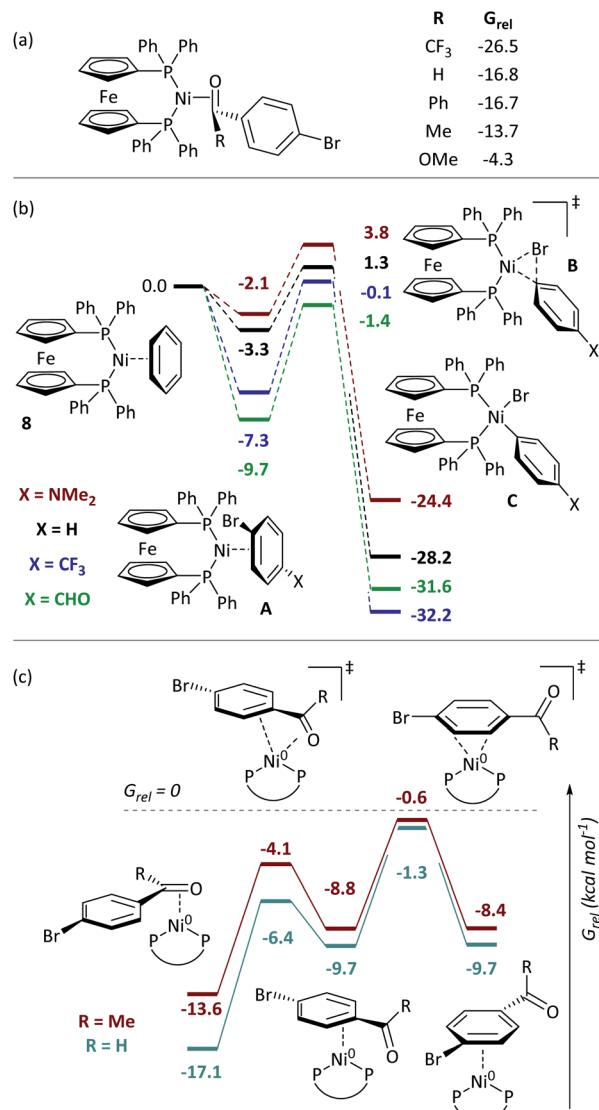


Fig. 4 (a) Coordination to aldehydes, ketones, and esters. (b) Free energy profile for oxidative addition. (c) Calculations on the ring-walking process. All energies are free energies in toluene solution and are quoted in  $\text{kcal mol}^{-1}$ .

with experiment, aldehydes and ketones coordinate  $[\text{Ni}(\text{dppf})]$  exergonically *via* the carbonyl group (Fig. 4(a)). Free energy profiles were calculated for the oxidative addition reactions of selected aryl bromides (Fig. 4(b));<sup>37</sup> reactions proceed *via* transition state B to irreversibly form  $\text{Ni}^{\text{II}}$  products C. The aldehyde substrate can also form the  $\eta^2(\text{CO})$  complex.

Further calculations were undertaken to model the ring-walking<sup>38–42</sup> step, using **2a-Br** and **3-Br** as substrates. In each case, three  $\eta^2$ -complexes are linked by two transition states, leading from the carbonyl group to the halide site (Fig. 4(c)). The transition states for these ring-walking steps are all lower in energy than **8** and so this process is more energetically favourable than the dissociation of the aryl halide and coordination of a new aryl halide; once an aldehyde- or ketone-containing substrate coordinates the nickel centre *via* the carbonyl ligand, it will undergo oxidative addition after ring walking,



rather than ligand exchange for an alternative substrate. Substrate **2c-Br** undergoes a similar ring-walking process, again with no intermediates or transition states that have  $G_{\text{rel}} > 0.8$ . These data are consistent with two key experimental observations: (i) the enhanced rate of oxidative addition, because  $\eta^2(\text{CO})$  coordination renders aldehyde- and ketone-containing aryl halides competitive ligands (*versus* COD); and (ii) selective cross-coupling, because aldehyde- and ketone-containing aryl halides are much better ligands for  $\text{Ni}^0$  than aryl halides without such strongly coordinating groups.

### Catalyst inhibition by aldehydes and ketones

The coordination of ketones and aldehydes to  $\text{Ni}^0$  might be expected to have a detrimental effect on the performance of cross-coupling reactions if this behaviour sequesters the active catalyst. A 'robustness screen'<sup>43,44</sup> was used, in which a model reaction was carried out in the presence of 1 equiv. of each of a series of additives (**9–19**).\*\* This provides a rapid and quantitative measure of the effect of each additive. A palette of additives was examined (Fig. 5).

Most additives had little effect on the reaction conversion. Aldehyde and ketone additives – except for acetophenone (**12**) – had a significant and detrimental effect, with the reaction almost completely ceasing when 1 equiv. of 2,2,2-trifluoroacetophenone (**15**) was present. The degree of inhibition of the reaction is correlated to  $K_{\text{eq}}$  for the displacement of COD from **1** (*vide supra*); it may be necessary to protect aldehydes and ketones in some reactions to prevent their coordination to  $\text{Ni}^0$ . If catalyst decomposition was responsible for the decrease in yield then we would expect that at the end of the reaction  $\geq 5\%$  of the additive would have been consumed;<sup>45</sup> in the case of **13** and **14**,  $\leq 2\%$  of the additive is unaccounted for, while **15** hydrates in the presence of water, resulting in the absence of 12–15% of **15** at the end of the reaction. There is no correlation between the degree of inhibition and the amount of additive unaccounted for.

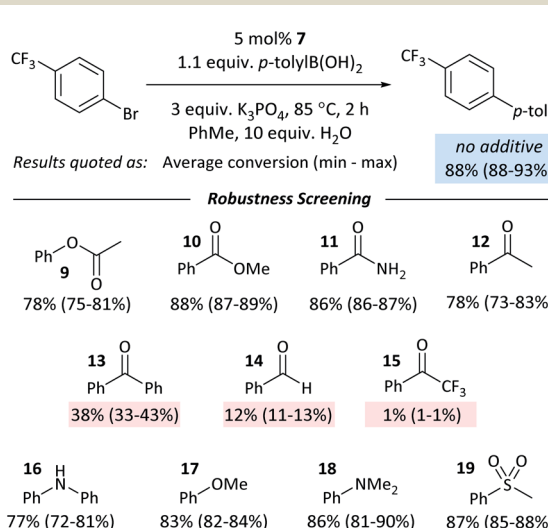
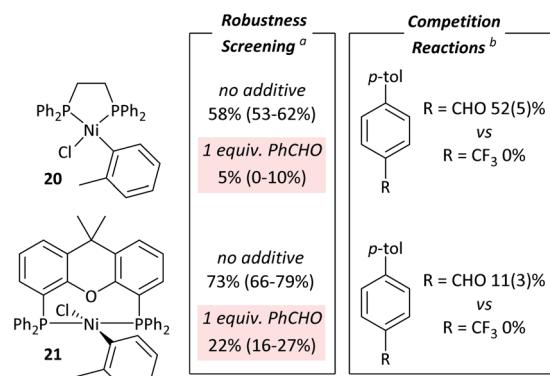


Fig. 5 Results from the robustness screen.



a) 5 mol% catalyst, 1 equiv. **5-Br**, 1.1 equiv. *p*-tolB(OH)<sub>2</sub>, 3 equiv. K<sub>3</sub>PO<sub>4</sub>, 10 equiv. H<sub>2</sub>O, PhMe, 85 °C, 2 h. b) 5 mol% catalyst, 1 equiv. **3-Br**, 1 equiv. **5-Br**, 1 equiv. *p*-tolB(OH)<sub>2</sub>, 3 equiv. K<sub>2</sub>PO<sub>4</sub>, 4:1 v/v THF/water, 85 °C, 2 h.

Fig. 6 Results with dppe and Xantphos catalysts.

Control experiments where one equivalent of benzaldehyde was added to the cross-coupling of **4-Cl** and *p*-tolylboronic acid showed complete conversion to the cross-coupling product. Aldehyde and ketone additives therefore have less of an effect on the cross-coupling reactions of aldehyde- and

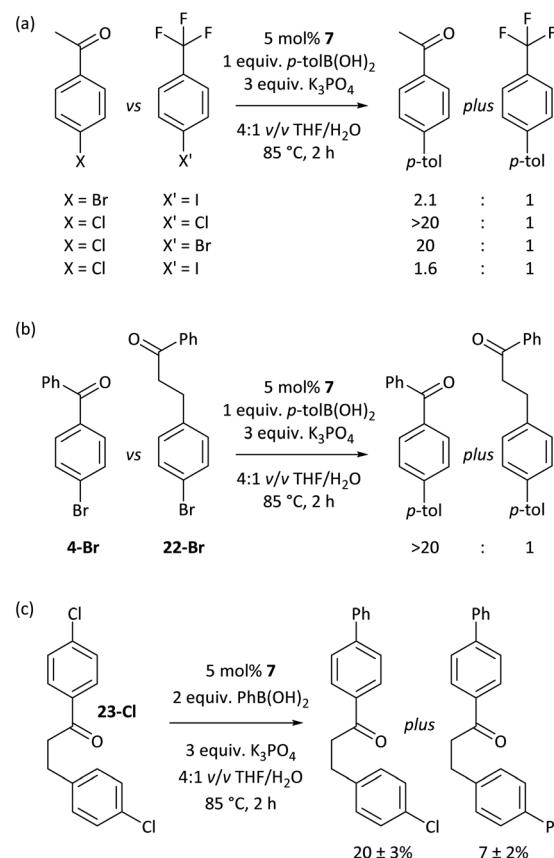


Fig. 7 (a) Overriding the intrinsic reactivity differences between aryl halides. (b) Selectivity between different carbonyl-containing substrates. (c) Site-selectivity within a molecule, enforced by carbonyl coordination.



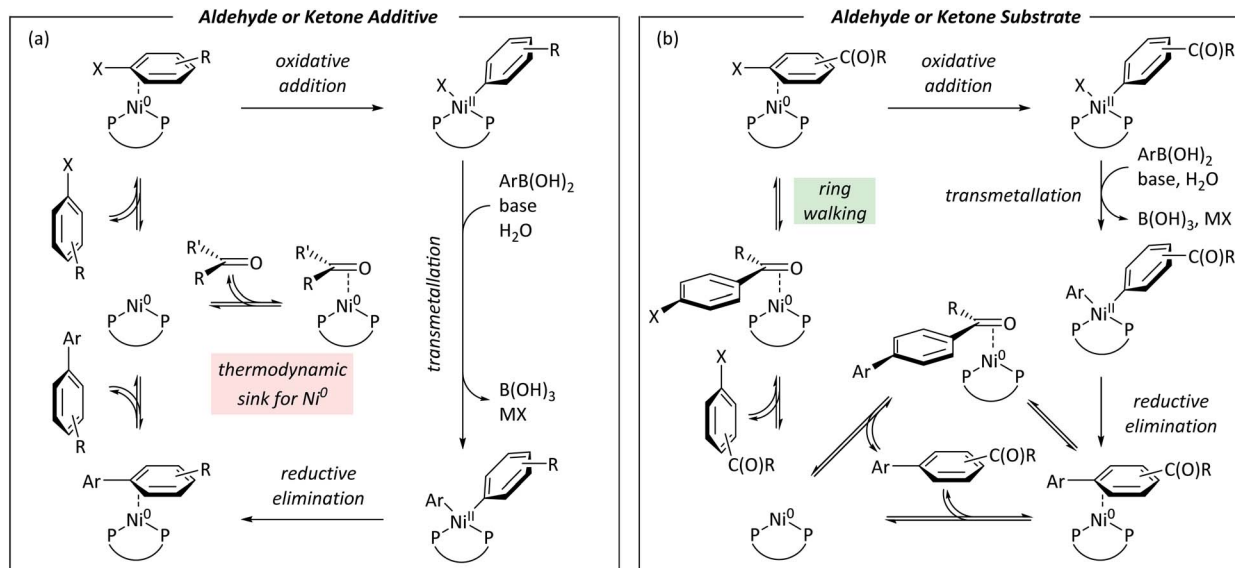


Fig. 8 (a) Catalytic cycle for nickel-catalysed Suzuki–Miyaura reactions in the presence of exogenous aldehyde or ketone. (b) Catalytic cycle for nickel-catalysed Suzuki–Miyaura reactions of aldehyde- and ketone-containing aryl halides.

ketone-containing aryl halides than they do on the cross-coupling of aryl halides that do not contain these functional groups.

The robustness screening data are consistent with coordination of an exogenous additive to the  $\text{Ni}^0$  catalyst inhibiting the reaction. No ring-walking is possible from such intermediates to a site for oxidative addition or other exergonic onward reaction.

### On the generality of these effects

These observations are not limited to dppf-based (pre)catalysts.  $[\text{NiCl}(\text{o-tol})(\text{L})_n]$  ( $\text{L} = \text{dppe}$  (20), Xantphos (21))<sup>34</sup> were applied in: (i) competition reactions between 5-Br and 3-Br, in which 3-Br reacts exclusively; and (ii) robustness screening reactions using 5-Br as the substrate and benzaldehyde as the additive, showing significant reaction inhibition (Fig. 6).<sup>††</sup> Complexes 20 and 21 perform significantly less well than 7 but may yield better results if further reaction optimisation was carried out. The results in Fig. 6 illustrate that the effect is general to nickel phosphine complexes, and not limited to dppf-based catalysts. Palladium, specifically  $[\text{PdCl}_2(\text{dppf})]$ , shows a far reduced propensity to undergo selective cross-coupling reactions, but has far better functional group tolerance.<sup>20</sup>

### Opportunities for exploitation

The carbonyl coordination effect was leveraged to achieve site selectivity in cross-coupling reactions, both intermolecularly and intramolecularly (Fig. 7). The aldehyde/ketone effect allows the normal reactivity order of aryl halides ( $\text{I} > \text{Br} > \text{Cl}$ )<sup>19</sup> to be entirely overridden, to the extent that an aryl chloride (2a-Cl) undergoes selective coupling in the presence of an electron-deficient aryl bromide (5-Br) and even in the presence of an aryl iodide (5-I) (Fig. 7(a)). Reactions are selective for aldehydes

over ketones, as judged from further competition experiments.<sup>§</sup> Ketones that are not in conjugation with the aryl halide  $\pi$ -system are not selectively coupled (e.g. 22-Br) (Fig. 7(b)). Intramolecular competition experiments were carried out using 23-Cl, which has two aryl chloride sites that are available for cross-coupling but only one is in conjugation with a ketone (Fig. 7(c)); reactions with 23-Cl establish that selective cross-coupling occurs at the site that is in conjugation with the ketone. Intrinsic differences in the reactivities of aryl chlorides, bromides, and iodides have been leveraged in the past for selective cross-coupling reactions,<sup>46</sup> but this work shows that the substitution pattern of the aryl halide can significantly change the order of reactivity, opening new avenues for creative organic synthesis using nickel-catalysed cross-coupling.

### Conclusions

This work establishes how aldehydes and ketones can have positive or negative effects on nickel-catalysed reactions, depending on their location. The formation of  $\eta^2$ -complexes has been implicated in some nickel-catalysed reactions<sup>30,31,39,47,48</sup> but this work shows that coordination effects can influence even simple and ubiquitous Suzuki–Miyaura reactions.

- Aryl halides with aldehyde and ketone functional groups undergo rapid oxidative addition because of favourable ligand exchange and ring-walking processes.
- Selectivity is achieved for aldehyde- or ketone-containing aryl halides over other aryl halide substrates because of this favourable coordination.
- Aldehydes and ketones that are present in cross-coupling reactions but are not in conjugation with the aryl halide act as inhibitors of catalysis.
- Aldehydes and ketone-containing aryl halides undergo successful cross-coupling.



Fig. 8 summarises the conclusions of this study using  $\text{Ni}^0/\text{Ni}^{\text{II}}$  cycles based on literature evidence from studies of nickel/dppf-catalysed reactions.<sup>18,19,49–53</sup> Fig. 8(a) shows a cycle for a reaction in which an aldehyde or ketone is present as an additive; a low energy  $\eta^2(\text{CO})$  complex sequesters the active catalyst and slows the reaction because the  $\eta^2$ -complex with the aryl halide is higher in energy. Fig. 8(b) shows a cycle for an aryl halide with an aldehyde or ketone substituent.

We are currently pursuing further work within our laboratories to understand the effects of a wider range of functional groups on nickel-catalysed reactions and their fundamental steps using kinetic and mechanistic studies.

## Conflicts of interest

There are no conflicts to declare.

## Acknowledgements

We are grateful for funding from: a Syngenta/Engineering and Physical Sciences Research Council (EPSRC) Industrial CASE Studentship for AKC (EP/P51066X/1); the EPSRC (EP/M027678/1); the University of Strathclyde for a Chancellor's Fellowship for DJN (2014–2018); and the Carnegie Trust for the Universities of Scotland for a Research Incentive Grant (RIG008165). We thank the Department of Pure and Applied Chemistry at the University of Strathclyde for consumables and facilities funding for DKL. We thank Mr G. Bain, Mr C. Irving, Ms P. Keating, and Dr J. Parkinson for assistance with technical and analytical facilities. We thank Dr J. Sanderson (University of Newcastle) for assistance with initial factorial experimental design studies. Some of the results reported here were obtained using the EPSRC-funded ARCHIE-WeSt high-performance computer (archie-west.ac.uk) (EP/K000586/1); we are grateful to Mr J. Buzzard, Dr K. Kubiak-Ossowska, and Dr R. Martin for their assistance with this facility. We thank Dr S. Sproules for EPR analyses and Dr A. Watson (University of St Andrews) for helpful discussions.

## Notes and references

\*\* Reaction outcomes were analysed using calibrated GC-FID analyses. In some competition experiments, total yield sometimes slightly exceeded 100% which is likely to be due to errors in weighing out exactly one equivalent of boronic acid.  
 †† Calculations were carried out using Gaussian09 Rev. D01.<sup>54</sup> Geometry optimisations were carried out without symmetry constraints using the B3LYP functional with Grimme's D3 dispersion corrections, the LANL2DZ(dp) basis set on Br and I, the LANL2TZ(f) basis set on Ni and Fe, and the 6-31G(d) basis set on all other atoms. The nature of stationary points was confirmed using frequency calculations. Energies were refined using single point calculations in which the 6-31G(d) basis set was exchanged for 6-311+G(d,p). All calculations were carried out in toluene solvent using the SMD solvent model.

- 1 S. Z. Tasker, E. A. Standley and T. F. Jamison, *Nature*, 2014, **509**, 299–309.
- 2 J. Twilton, P. Zhang, M. H. Shaw, R. W. Evans and D. W. MacMillan, *Nat. Rev. Chem.*, 2017, **1**, 0052.
- 3 J. C. Tellis, C. B. Kelly, D. N. Primer, M. Jouffroy, N. R. Patel and G. A. Molander, *Acc. Chem. Res.*, 2016, **49**, 1429–1439.

- 4 D. J. Weix, *Acc. Chem. Res.*, 2015, **48**, 1767–1775.
- 5 T. Mesganaw and N. K. Garg, *Org. Process Res. Dev.*, 2012, **17**, 29–39.
- 6 T. Schaub, M. Backes and U. Radius, *J. Am. Chem. Soc.*, 2006, **128**, 15964–15965.
- 7 M. Tobisu, T. Xu, T. Shimasaki and N. Chatani, *J. Am. Chem. Soc.*, 2011, **133**, 19505–19511.
- 8 J. E. Dander and N. K. Garg, *ACS Catal.*, 2017, **7**, 1413–1423.
- 9 C. Y. Lin and P. P. Power, *Chem. Soc. Rev.*, 2017, **46**, 5347–5399.
- 10 J. Jover, *Catal. Sci. Technol.*, 2019, **9**, 5962–5970.
- 11 T. Inatomi, Y. Fukahori, Y. Yamada, R. Ishikawa, S. Kanegawa, Y. Koga and K. Matsubara, *Catal. Sci. Technol.*, 2019, **9**, 1784–1793.
- 12 G. D. Jones, J. L. Martin, C. McFarland, O. R. Allen, R. E. Hall, A. D. Haley, R. J. Brandon, T. Konovalova, P. J. Desrochers, P. Pulay and D. A. Vicic, *J. Am. Chem. Soc.*, 2006, **128**, 13175–13183.
- 13 I. Funes-Ardoiz, D. J. Nelson and F. Maseras, *Chem.-Eur. J.*, 2017, **23**, 16728–16733.
- 14 D. J. Nelson and F. Maseras, *Chem. Commun.*, 2018, **54**, 10646–10649.
- 15 K. Zhang, M. Conda-Sheridan, S. R. Cooke and J. Louie, *Organometallics*, 2011, **30**, 2546–2552.
- 16 D. S. McGuinness, K. J. Cavell, B. W. Skelton and A. H. White, *Organometallics*, 1999, **18**, 1596–1605.
- 17 A. Manzoor, P. Wienefeld, M. C. Baird and P. H. M. Budzelaar, *Organometallics*, 2017, **36**, 3508–3519.
- 18 G. Yin, I. Kalvet, U. Englert and F. Schoenebeck, *J. Am. Chem. Soc.*, 2015, **137**, 4164–4172.
- 19 S. Bajo, G. Laidlaw, A. R. Kennedy, S. Sproules and D. J. Nelson, *Organometallics*, 2017, **36**, 1662–1672.
- 20 A. K. Cooper, P. M. Burton and D. J. Nelson, *Synthesis*, 2020, DOI: 10.1055/s-0039-1690045.
- 21 We have established the mechanism of this reaction, and showed that this proceeds *via* oxidative addition to form  $\text{Ni}^{\text{II}}$  intermediates – which are only observable when the aryl halide has *ortho*-substituents – which then undergo comproportionation to  $\text{Ni}(0)$ . Please see ref. 19 for details.
- 22 C. Hansch, A. Leo and R. W. Taft, *Chem. Rev.*, 1991, **91**, 165–195.
- 23 D. Walther, *Z. Anorg. Allg. Chem.*, 1977, **431**, 17–30.
- 24 D. Walther, *J. Organomet. Chem.*, 1980, **190**, 393–401.
- 25 J. Kaiser, J. Sieler, D. Walther, E. Dinjus and L. Golic, *Acta Crystallogr., Sect. B: Struct. Sci.*, 1982, **38**, 1584–1586.
- 26 R. Countryman and B. R. Penfold, *J. Cryst. Mol. Struct.*, 1972, **2**, 281–290.
- 27 T. T. Tsou, J. C. Huffman and J. K. Kochi, *Inorg. Chem.*, 1979, **18**, 2311–2317.
- 28 A. Flores-Gaspar, P. Pinedo-González, M. G. Crestani, M. Muñoz-Hernández, D. Morales-Morales, B. A. Warsop, W. D. Jones and J. J. García, *J. Mol. Catal. A: Chem.*, 2009, **309**, 1–11.
- 29 R. Doi, K. Kikushima, M. Ohashi and S. Ogoshi, *J. Am. Chem. Soc.*, 2015, **137**, 3276–3282.
- 30 C. Lei, Y. J. Yip and J. S. Zhou, *J. Am. Chem. Soc.*, 2017, **139**, 6086–6089.



31 Y. Hoshimoto, M. Ohashi and S. Ogoshi, *Acc. Chem. Res.*, 2015, **48**, 1746–1755.

32 A. N. Desnoyer, W. He, S. Behyan, W. Chiu, J. A. Love and P. Kennepohl, *Chemistry*, 2019, **25**, 5259–5268.

33 W. He and P. Kennepohl, *Faraday Discuss.*, 2019, **220**, 133–143.

34 E. A. Standley, S. J. Smith, P. Müller and T. F. Jamison, *Organometallics*, 2014, **33**, 2012–2018.

35 Equivalent data are obtained in a THF/water solvent mixture; please see ref. 16.

36 Control experiments with ketone-functionalised boronic acids did not lead to selective cross-coupling of these species (see the ESI§). Coordination occurs to Ni(0) only, and not to the more sterically-crowded and less electron-rich Ni(II) intermediates.

37 Free energy profiles for the corresponding reactions of a wider range of aryl halides can be found in the ESI§.

38 N. Yoshikai, H. Matsuda and E. Nakamura, *J. Am. Chem. Soc.*, 2008, **130**, 15258–15259.

39 L. Guo, S. Dai, X. Sui and C. Chen, *ACS Catal.*, 2016, **6**, 428–441.

40 O. V. Zenkina, A. Karton, D. Freeman, L. J. W. Shimon, J. M. L. Martin and M. E. van der Boom, *Inorg. Chem.*, 2008, **47**, 5114–5121.

41 J. A. Bilbrey, A. N. Bootsma, M. A. Bartlett, J. Locklin, S. E. Wheeler and W. D. Allen, *J. Chem. Theory Comput.*, 2017, **13**, 1706–1711.

42 S. K. Sontag, J. A. Bilbrey, N. E. Huddleston, G. R. Sheppard, W. D. Allen and J. Locklin, *J. Org. Chem.*, 2014, **79**, 1836–1841.

43 K. D. Collins and F. Glorius, *Acc. Chem. Res.*, 2015, **48**, 619–627.

44 K. D. Collins and F. Glorius, *Nat. Chem.*, 2013, **5**, 597–601.

45 This assumes a >1 : 1 additive : nickel stoichiometry in such a decomposition reaction, based on the low concentrations of nickel in the reactions and the high concentrations of additive (20 equiv. with respect to nickel).

46 C. P. Seath, J. W. B. Fyfe, J. J. Molloy and A. J. B. Watson, *Angew. Chem., Int. Ed.*, 2015, **54**, 9976–9979.

47 E. L. Lanni and A. J. McNeil, *J. Am. Chem. Soc.*, 2009, **131**, 16573–16579.

48 W. He, B. O. Patrick and P. Kennepohl, *Nat. Commun.*, 2018, **9**, 3866.

49 L. M. Guard, M. Mohadjer Beromi, G. W. Brudvig, N. Hazari and D. J. Vinyard, *Angew. Chem., Int. Ed.*, 2015, **54**, 13352–13356.

50 I. Kalvet, Q. Guo, G. J. Tizzard and F. Schoenebeck, *ACS Catal.*, 2017, **7**, 2126–2132.

51 M. Mohadjer Beromi, A. Nova, D. Balcells, A. M. Brasacchio, G. W. Brudvig, L. M. Guard, N. Hazari and D. J. Vinyard, *J. Am. Chem. Soc.*, 2017, **139**, 922–936.

52 M. Mohadjer Beromi, G. Banerjee, G. W. Brudvig, N. Hazari and B. Q. Mercado, *ACS Catal.*, 2018, **8**, 2526–2533.

53 M. Mohadjer Beromi, G. Banerjee, G. W. Brudvig, D. J. Charboneau, N. Hazari, H. M. C. Lant and B. Q. Mercado, *Organometallics*, 2018, **37**, 3943–3955.

54 M. J. Frisch, G. W. Trucks, H. B. Schlegel, G. E. Scuseria, M. A. Robb, J. R. Cheeseman, G. Scalmani, V. Barone, G. A. Petersson, H. Nakatsuji, X. Li, M. Caricato, A. Marenich, J. Bloino, B. G. Janesko, R. Gomperts, B. Mennucci, H. P. Hratchian, J. V. Ortiz, A. F. Izmaylov, J. L. Sonnenberg, D. Williams-Young, F. Ding, F. Lipparini, F. Egidi, J. Goings, B. Peng, A. Petrone, T. Henderson, D. Ranasinghe, V. G. Zakrzewski, J. Gao, N. Rega, G. Zheng, W. Liang, M. Hada, M. Ehara, K. Toyota, R. Fukuda, J. Hasegawa, M. Ishida, T. Nakajima, Y. Honda, O. Kitao, H. Nakai, T. Vreven, K. Throssell, J. A. Montgomery Jr, J. E. Peralta, F. Ogliaro, M. Bearpark, J. J. Heyd, E. Brothers, K. N. Kudin, V. N. Staroverov, T. Keith, R. Kobayashi, J. Normand, K. Raghavachari, A. Rendell, J. C. Burant, S. S. Iyengar, J. Tomasi, M. Cossi, J. M. Millam, M. Klene, C. Adamo, R. Cammi, J. W. Ochterski, R. L. Martin, K. Morokuma, O. Farkas, J. B. Foresman and D. J. Fox, *Gaussian 09, Revision D.01*, Gaussian, Inc., Wallingford CT, 2016.

